PHYSICAL REVIEW D **86,** 026010 (2012)

Holographic D instanton liquid and chiral transition

Bogeun Gwak,[1,2,*] Minkyoo Kim,[1,2,†] Bum-Hoon Lee,[1,2,‡] Yunseok Seo,[2,§] and Sang-Jin Sin[3,‖]

[1]*Department of Physics, Sogang University, Seoul 121-742, Korea*
[2]*Center for Quantum Spacetime, Sogang University, Seoul 121-742, Korea*
[3]*Department of Physics, Hanyang University, Seoul 133-791, Korea*

(Received 27 March 2012; published 25 July 2012)

We study the phase diagram of *black* D3 geometry with uniformly distributed D-instanton charge using the probe D7 brane. In the presence of uniform D-instanton charges, quarks can be confined, although gluons are not, because baryon vertices are allowed due to the net repulsive force on the on the probe D-branes. Since there is no scale in the geometry itself apart from the horizon size, there is no Hawking-Page transition. As a consequence, the D7 brane embedding can encode the effect of the finite temperature as well as finite baryon density even for low temperature. The probe D-brane embedding, however, undergoes a phase transition which can be interpreted as a chiral transition as we change temperature and density. We studied such phase transitions and calculated the constituent quark mass, chiral condensation, and the binding energy of baryons as function of the density. The baryon vertex melting is identified as the quark deconfinement. We draw the phase diagram according to these transitions.

DOI: 10.1103/PhysRevD.86.026010 PACS numbers: 11.25.Tq

I. INTRODUCTION

One of the difficulties in holographic QCD is to discuss the temperature dependence of physical observables in the hadron phase. The problem is the presence of the Hawking-Page transition as the deconfinement/confinement transition [1]; the background metric describing the low-temperature phase does not contain any temperature parameter. Describing the hadrons in finite temperature requires having a black hole metric, in which gluons are always deconfined. Therefore, we are lead to the question whether a quark can be confined while gluons are deconfined. In fact, the degrees of freedom of two species are different in large N_c order, and the confinement of gluons and that of quarks should be separate phenomena at least in the large N_c limit. However, in most of the geometric background with well-defined Hawking temperature, a baryon vertex [2] is not allowed as a finite energy solution [3,4] because a black D-brane has net attractive gravity.

To have a phase transition, we need a scale other than the temperature. In QCD, scale invariance is broken by the chiral and gluon condensation, and it is also known that both of them can be induced by the instanton effect. In fact, there has been huge activity to utilize the instanton background. The topic directly relevant to our paper is the instanton gas/liquid model, where mass generation and the chiral symmetry breaking is discussed using chiral anomaly and fermion zero modes. For a review, see the article by Schafer and Shuryak [5] and references therein.

It is also well-known that the D-instanton is the gravity dual to the Yang-Mills instanton. Therefore, it is very natural to try to use a gravity background dual to the instanton gas. In fact, Hong Liu and Tseytlin, in Ref. [6], proposed that the D3/D-instanton geometry where D-instanton is uniformly distributed over D3, is dual of the $N = 4$ Yang-Mills theory with constant gluon condensation but zero electric/magnetic gluon field, which is $\langle F_{\mu\nu}\rangle = 0$, $\langle \mathrm{Tr} F^{\mu\nu}F_{\mu\nu}\rangle = cq \neq 0$, where F is field strength of the gauge fields. Such D3/D-instanton geometry contains a nontrivial dilaton giving a nonzero value of gluon condensation q, which was identified precisely as the D-instanton density.

While the chiral symmetry breaking was a natural consequence of the instanton background, the confinement was not easy to show with the instanton gas model. One of the interesting consequences of the AdS/CFT is that it is easy to show that the dual gauge theory of the D3/D-instanton background has a confinement property with the linear quark-antiquark potential. Therefore, both the chiral condensation and confinement turn out to be consequences of the presence of the D-instanton charge, which effectively produces net repulsive force on the probe D-branes and the fundamental strings.

The purpose of this paper is to consider the finite temperature and density of the holographic dual of the D-instanton gas/liquid. For our purpose, we need to extend the geometry of Liu and Tseytlin to the finite temperature case. The necessary metric was found by Ghoroku *et al.* [7] in the context completely unrelated to the instanton gas model. While most of the dilaton gravity solution is singular [8,9] such that temperature is ill-defined, the solution in Ref. [7] allows a Hawking temperature. The geometry is quasiconfining; namely, it has the following properties [7]:

*rasenis@sogang.ac.kr
†mkim80@sogang.ac.kr
‡bhl@sogang.ac.kr
§yseo@sogang.ac.kr
‖sjs@hanyang.ac.kr

(i) gluons are deconfined: In QCD, one can consider the gluon propagator directly and state the (de)confinement. However, in holographic QCD, one cannot look at the gluon propagator directly since that is a colored object whose treatment is beyond the gravity limit. Instead, what one should look at is the spectrum of the dilaton field which is the dual of the glueball operator. If that spectral function has well-defined peaks, this is the signal of confinement. If it does not show any peak, it means glueballs are all disintegrated and the system is in a deconfined phase. The presence of the horizon does not allow any stable glueball spectrum because it is known that the quasinormal mode in an AdS black hole has a large imaginary part.

(ii) the quark-anti quark potential is Coulomb-like for short distance, linear for medium distance, and constant for large enough distances. The turnover points depend on temperature and gluon condensation.

(iii) A baryon vertex solution is allowed in a low enough temperature.

It is important to notice that in this background, there is no geometric transition as temperature grows. This is because (i) we do not have any compactified direction, (ii) we need to work out the thermodynamics of the bulk theory in Einstein frame, in which our geometry is the same as the black D3 brane, and (iii) the action for the dilaton and axion cancel each other. The difference between the black D3 brane with and without D-instantons comes from the probe D-brane dynamics, which should be calculated in the string frame where the dilaton factor is manifest as an overall factor in the metric.

It turns out that the Chern-Simons (CS) term cannot cancel the effect of the dilaton unlike the claim of Ref. [7], which is the origin of the chiral symmetry breaking in our paper. On the other hand, in Ref. [7], embedding is flat, and there is no chiral condensation. The flat embedding was attributed to the cancellation of the dilaton effect by the CS term. However, as we have shown in Appendix A, cancellation does not happen, and, therefore, brane embedding cannot be flat, which in turn induces the chiral symmetry breaking. We attribute such an effect to the net repulsive force acting on probe D7 created by the D-instanton charges. Such breaking of the chiral symmetry is consistent with the gauge theory where the zero mode of the fermions in the D-instanton background requires chiral symmetry breaking.

For the treatment of chemical potential, we follow the method first suggested in Refs. [10,11] and developed in Refs. [12,13]. There are two types of probe-brane embedding. One describes quark phase, where the flavor brane touches the black-hole horizon, and a baryon vertex is not allowed. Usually this embedding is called *black hole embedding*. If there are strings connecting the horizon and the D7, the latter is deformed to a spiky brane to touch the horizon. The other embedding is the one where D7 brane never touches the horizon. On such a brane, strings can be attached only if a baryon vertex is allowed and present so that the strings connect the baryon vertex to D7. We find that there is a phase transition between two embeddings. We also find that there is a transition between the two black-hole embeddings. The binding energy of the baryon and the melting temperature in this background was studied in Refs. [14,15] by considering one baryon vertex connected to the boundary at infinity by N_c strings. We treat the baryonic medium using the method developed in Ref. [4] where each compact baryon vertex is joined with a D7 probe brane through a funnel, and such a configuration is smeared along the D3 direction.

One final comment here is about the nomenclature: usually, instanton gas is for a weakly interacting far-separated instanton, and liquid is for dense and nontrivial interaction. Here, we are using the words ''instanton liquid'' since homogenous distribution would not be consistent with the well-separated gas configuration. We do not focus on the interaction strength at all. Also, instanton liquid is a name to denote a phenomenological model assuming a certain size and distribution of instantons. While we aim to discuss the dual of this model, there are differences in detail. Therefore, it is better to call our model a D-instanton liquid.

The rest of the paper is planned as follows. In Sec. II, the background geometry is reviewed, and various embedding configurations were studied with zero density, and chiral condensations are calculated. In Sec. III, we study how the embedding geometry changes as we vary 3 parameters: temperature, baryon/quark density, and the gluon condensation. We find that there can be two phases within quark phase: one chiral symmetry broken and the other chiral symmetry restored. In Sec. IV, by calculating the free energy and chemical potential as a function of density, we study the phase transition between the baryon and quark phases as well as the phase transition between the two quark phases. We work out the complete phase diagram both in canonical and grand canonical ensemble. In Sec. VI, we give a conclusion and future directions. In Appendix A, we show that the CS term cannot cancel the effect of the dilaton unlike the Ref. [7].

II. BACKGROUND GEOMETRY AND D-BRANE SETUP

Here, we will briefly review the background geometry and the probe-brane setup within it. The geometry is the one which is a finite temperature extension of D3/D-instanton background with Euclidean signature given by Ref. [7]. The background has a fiveform field strength and a axion field which couples to the D3 and D-instanton, respectively. The ten-dimensional supergravity action in the Einstein frame is given by Refs. [16,17]

$$S = \frac{1}{\kappa}\int d^{10}x\sqrt{g}\left(R - \frac{1}{2}(\partial\Phi)^2 + \frac{1}{2}e^{2\Phi}(\partial\chi)^2 - \frac{1}{6}F_{(5)}^2\right), \tag{2.1}$$

where Φ and χ denote the dilaton and the axion, respectively. If we set $\chi = -e^{-\Phi} + \chi_0$, the dilaton term cancels the axion term in Eq. (2.1). Then, the action becomes that of the metric and fiveform. The solution in string frame can be written as [18]

$$\begin{aligned} ds_{10}^2 &= e^{\Phi/2}\left[\frac{r^2}{R^2}(f(r)^2dt^2 + d\vec{x}^2) + \frac{1}{f(r)^2}\frac{R^2}{r^2}dr^2 + R^3 d\Omega_5^2\right], \\ e^{\Phi} &= 1 + \frac{q}{r_T^4}\log\frac{1}{f(r)^2}, \qquad \chi = -e^{-\Phi} + \chi_0, \\ f(r) &= \sqrt{1 - \left(\frac{r_T}{r}\right)^4}, \end{aligned} \tag{2.2}$$

where $R^4 = 4\pi g_s N_c \alpha'^2$. The constant q denotes the number of D-instantons. From the AdS/CFT dictionary, it also represents the vacuum expectation value of gluon condensation. The dilaton factor diverges at the black-hole horizon. However, it does not give any effect on the thermodynamics of the *bulk theory* since the latter should be calculated in the Einstein frame where its on-shell action is the same as that of the black D3-brane solution. The geometry has a regular event horizon and Hawking temperature given by $T = r_T/\pi R^2$.

Quark-antiquark potential is derived from the expectation value of a Wilson loop using a U-shaped fundamental string configuration [7]. For a given temperature T, the U-shaped string touches the black hole horizon and splits into two straight strings at certain separation $L_*(T)$. This critical distance L_* increases as temperature decreases as in the usual black-hole geometry. The geometry corresponds to a deconfined phase from the gluon point of view. In usual black D3-brane geometry, $q\bar{q}$ potential is Coulomb-like for small separation and flat when separation is larger than L_*, where it is completely screened. In this background, the potential is Coulomb-like at short distances but linearly grows until the U-shaped string touches the horizon. At zero temperature, the potential is linear up to an indefinitely large distance. This is a similarity to the real QCD. But the gluon is deconfined, which is different from the real QCD. We call such phenomena "quasiconfinment". Such a quasiconfining property comes from the presence of q, which is the value of gluon condensation. It is the D-instanton number, and it should be closely related to the chiral condensation as well as the gluon condensation.

Introducing a dimensionless coordinate ξ by $\frac{d\xi^2}{\xi^2} = \frac{dr^2}{r^2 f^2(r)}$, the background geometry can be rewritten as

$$ds^2 = e^{\Phi/2}\left[\frac{r^2}{R^2}(f(r)^2dt^2 + d\vec{x}^2) + \frac{R^2}{\xi^2}(d\xi^2 + \xi^2 d\Omega_5^2)\right], \tag{2.3}$$

where r and ξ are related by

$$\begin{aligned} \left(\frac{r}{r_T}\right)^2 &= \frac{1}{2}\left(\frac{\xi^2}{\xi_T^2} + \frac{\xi_T^2}{\xi^2}\right), \quad \text{and} \quad f = \left(\frac{1 - \xi_T^4/\xi^4}{1 + \xi_T^4/\xi^4}\right) \equiv \frac{\omega_-}{\omega_+}, \\ \omega_\pm &\equiv 1 \pm \frac{\xi_T^4}{\xi^4}. \end{aligned} \tag{2.4}$$

To describe the embedding of the probe the D7-brane, we decompose the $\mathbb{R}^6$ part in Eq. (2.3) into $\mathbb{R}^4 \times \mathbb{R}^2$,

$$\begin{aligned} ds^2 = e^{\Phi/2}\Bigg[&\frac{r^2}{R^2}(f(r)^2dt^2 + d\vec{x}^2) + \frac{R^2}{\xi^2}(d\rho^2 + \rho^2\Omega_3^2 \\ &+ dy^2 + y^2 d\phi^2)\Bigg]. \end{aligned} \tag{2.5}$$

The D7-brane spans $(t, \vec{x}, \rho)$ direction and wraps S^3 and is perpendicular to the y and ϕ direction. We can set $\phi = 0$ using the $SO(2)$ symmetry in the x^8, x^9 plane. Then, the induced metric on the D7-brane becomes

$$\begin{aligned} ds_{D7}^2 = e^{\Phi/2}\Bigg[&\frac{r^2}{R^2}(f(r)^2dt^2 + d\vec{x}^2) \\ &+ \frac{R^2}{\xi^2}((1 + y'^2)d\rho^2 + \rho^2\Omega_3^2)\Bigg], \end{aligned} \tag{2.6}$$

where y' denotes $\partial y(\rho)/\partial\rho$ and $\xi^2 = \rho^2 + y^2$.

The general action of the probe D7-brane can be written as sum of Dirac-Born-Infeld (DBI) action of the D7-brane and the Chern-Simons term. The embedding dynamics of the D7-brane gives the dependence of the chiral condensation on control parameters like temperature, density, quark mass, etc., as we will describe below.

III. CHIRAL CONDENSATION AT ZERO DENSITY

Here, we study D7-brane embeddings at zero density, but we first consider the zero-temperature and zero-density case to study q dependence of the chiral condensation and then consider the finite temperature to study the chiral phase transition temperature as a function of gluon condensation.

A. Zero-temperature limit

In this limit, 10-dimensional geometry (2.2) becomes near-horizon geometry of a D3/D-instanton system which preserves half of supersymmetry [6],

$$\begin{aligned} ds^2 &= e^{\Phi/2}\left[\frac{r^2}{R^2}(dt^2 + d\vec{x}^2) + \frac{R^2}{r^2}(dr^2 + r^2 d\Omega_5^2)\right], \\ e^{\Phi} &= 1 + \frac{q}{r^4}, \qquad \chi = -e^{-\Phi} + \xi_\infty. \end{aligned} \tag{3.1}$$

The induced metric on the D7-brane can be written as

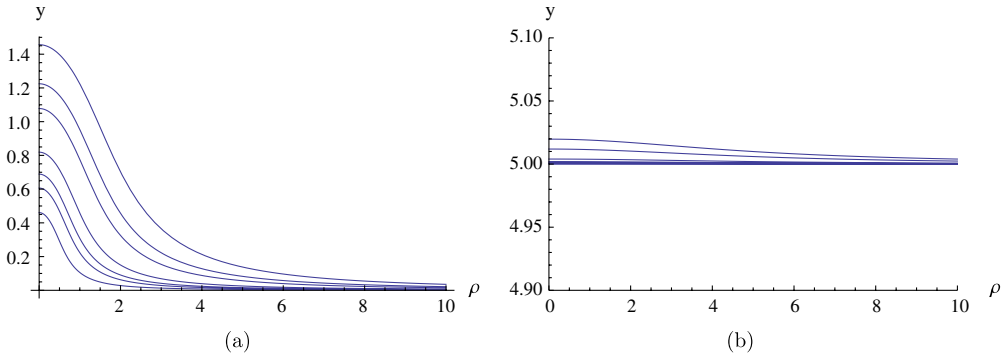

FIG. 1 (color online). (a) D7-brane embeddings for $m_q = 0$ with $q = 0$, 0.1, 0.3, 0.5, 1, 3, 5, 10 from bottom to top. (b) D7-brane embeddings for $m_q = 5$ with $q = 0$, 0.1, 0.3, 0.5, 1,3, 5, 10 from bottom to top.

$$ds^2_{D7} = e^{\Phi/2}\left[\frac{r^2}{R^2}(dt^2 + d\vec{x}^2) + \frac{R^2}{r^2}((1 + y'^2)d\rho^2 + \rho^2 d\Omega_3^2)\right], \tag{3.2}$$

where $r^2 = \rho^2 + y^2$. The presence of a D-instanton implies that of an axion. The axion can couple to the D7-brane world volume through the Chern-Simons term. Therefore, D7-brane action can be written as

$$\begin{aligned} S_{D7} &= S_{\mathrm{DBI}} + S_{\mathrm{CS}} \\ &= -\mu_7 \int d\sigma^8 e^{-\Phi}\sqrt{-\det(g + 2\pi\alpha' F)} \\ &\quad + \mu_7 \int d^8\sigma \frac{1}{8!} C_{(8)i_1\cdots i_8}, \end{aligned} \tag{3.3}$$

where σ is world volume coordinates of the D7-brane, g is the induced metric on the D7-brane, and $C_{(8)}$ is the Hodge dual 8-form gauge potential of the axion field which is 0-form. If we fix the D7-brane position along the fixed ϕ direction, the Chern-Simons term becomes locally total derivative as we prove in Appendix A. Therefore, it cannot affect the equation of motion; hence, we can ignore the Chern-Simons term. This observation makes the key difference of our D7-brane embedding compared to the one described in Ref. [7], and it will be the origin of the chiral symmetry breaking.

Now, the DBI action for the D7-brane can be written as

$$S_{D7} = -\tau_7 \int d\rho d\rho e^{\Phi}\rho^3\sqrt{1 + y'^2}, \tag{3.4}$$

with $\tau_7 = \mu_7 V_3 \Omega_3$, and the equation of motion is

$$\frac{d}{d\rho}\left(\frac{e^{\Phi}\rho^2 y'}{\sqrt{1 + y'^2}}\right) + \frac{q \cdot y\rho^3 e^{\Phi}\sqrt{1 + y'^2}}{r^6} = 0. \tag{3.5}$$

For a generic value of q, an analytic solution is not available. So we look for a numerical one. For $q = 0$, the trivial embedding $y =$ constant is a solution which is consistent with the result in Ref. [19].

If we turn on q, the solution deforms. The bare quark mass m_q and chiral condensation c are encoded in the asymptotic form of embedding function $y(\rho)$ [20,21]:

$$y(\rho) = m_q + \frac{c}{\rho^2} + \cdots. \tag{3.6}$$

The embeddings with fixed m_q are drawn in Fig. 1. As q increases, probe D7-brane in the central region bends upward more and more so that we have nonvanishing chiral condensation which is an increasing function of q. The value q corresponds to the gluon condensation $\langle \mathrm{Tr}F^2 \rangle$ in boundary theory and hence plays the role of parameter of scale symmetry breaking. The m_q dependence of chiral condensation is drawn in Fig. 2(a). With nonzero value of

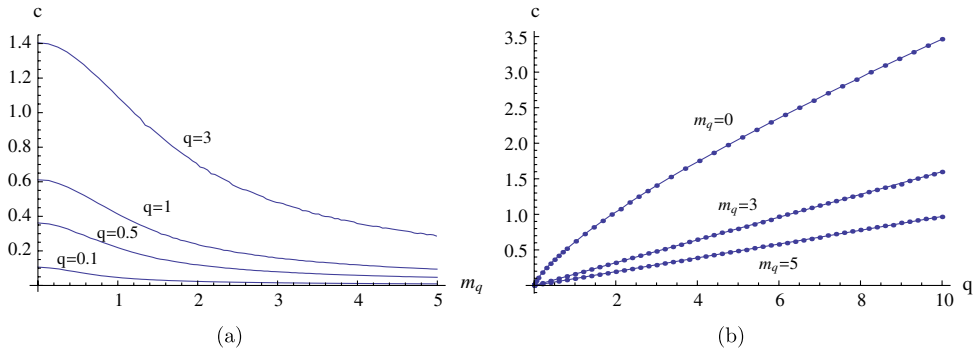

FIG. 2 (color online). (a) m_q dependence of chiral condensation with fixed q. (b) q dependence of chiral condensation with fixed m_q.

q, the value of chiral condensation goes to a finite value in ($m_q \to 0$). Therefore, the chiral symmetry is broken. The q dependences of the chiral condensation for given m_q are drawn in Fig. 2(b). The condensation is an increasing function of q but a decreasing one of m_q. At large quark mass, chiral condensation is linearly in q. It is consistent with the expectation from field theory [21–23],

$$\langle \bar{\psi}\psi \rangle = \frac{\alpha_s N_f}{12\pi m_q}\langle \mathrm{Tr}F^2 \rangle. \tag{3.7}$$

B. Finite temperature without density

In this section, we will study D7-brane embedding in black-hole geometry without chemical potential. We use the black-hole metric (2.2) and induce the metric on the D7-brane with Eq. (2.6). Then, DBI action for the D7-brane becomes

$$S_{D7} \equiv \tau_7 \int dt d\rho V(\rho, y)\sqrt{1+y'^2}, \tag{3.8}$$

where $\tau_7 = \xi_T^4 \mu_7 V_3 \Omega_3$ and $V = e^{\Phi}\rho^3 \omega_+ \cdot \omega_-$. The dilaton factor seems to diverge at the black-hole horizon. However, the dilaton factor e^{Φ} comes with ω_- which contains the zero $\sim(r - r_T)$ at the horizon. This zero is enough to kill the logarithmic divergence of the dilaton. In other words, the dilaton's log singularity does not change the qualitative behavior of the brane dynamics near the horizon.

The equation of motion for the DBI action can be written following form:

$$\frac{y''}{1+y'^2} + \frac{\partial \log V}{\partial \rho}y' - \frac{\partial \log V}{\partial y} = 0. \tag{3.9}$$

This equation of motion is highly nonlinear. We can get the solution only in a numerical way with the proper boundary condition (BC). In the presence of a black-hole horizon, embedding of probe D7 can be classified as "Minkokwski embedding" and "black-hole embedding" [24]. For the Minkowski embedding, we impose the BC: $y(0) = y_0$ and $y'(0) = 0$. For the black-hole embedding, the BC is determined by the regularity condition of the equation of motion at the horizon:

$$y(\rho_{\min}) = y_0, \qquad y'(\rho_{\min}) = \tan\theta, \tag{3.10}$$

where θ is the angle between the ρ axis and probe-brane position at the horizon. In usual black-hole geometry, gravitational attraction of a black hole bends the probe brane downward. However, a nonzero value of q gives net "repulsive" force on probe D7. Therefore, D7 bends upward. q dependences of Minkowski embedding and black-hole embedding are drawn in Fig. 3. For fixed quark mass and temperature, the bigger q is, the more pushed up the D7 brane is. Such an effect is common both in Minkowski and black-hole embedding.

We expect a phase transition between Minkowski and black-hole embeddings as we increase temperature. Namely, Minkowski embedding in low temperature will change into black-hole embedding in high temperature. In the presence of q, D7 feels repulsive force; therefore, we expect that as q increases, phase-transition temperature goes up. One may expect that the phase transition might be smoother compared with the case of no instanton charge. One can extract the q dependence of phase-transition temperature ξ_T^* from the free energy. The case for $m_q = 1$ is drawn in Fig. 4.

Now, we will discuss chiral condensation for this system: it was defined as the slope of D7-brane at the asymptotic region. See Eq. (3.6). We first fix the temperature and calculate it with different m_q's. For $q = 0$, the D7-brane bends down, its slope at the asymptotic region is positive, and therefore, the condensation value is negative. See Fig. 5(a). If we turn on q and increase it slowly, the brane bends up a relatively very small value of q since the pushing-up effect of q is very effective. Therefore, the sign of the condensation flips at a small value of q. Also, the value of m_q where phase transition occurs decreases as q increases.

As we decrease m_q with fixed q, there is phase transition from Minkowski embedding to black-hole embedding at a certain value of m_q. See Fig. 5. In Figs. 5(e) and 5(f), there is range where m_q becomes negative. If we calculate free energy, there is phase transition before m_q becomes

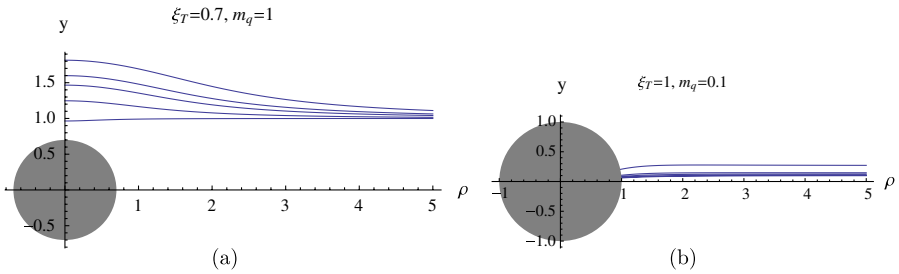

FIG. 3 (color online). (a) q dependence of Minkowski embedding for $m_q = 1$ with $q = 0, 1, 3, 5, 10$ from below. (b) q dependence of black hole embedding for $m_q = 0.1$ with $q = 0, 1, 3, 5, 10$ from below.

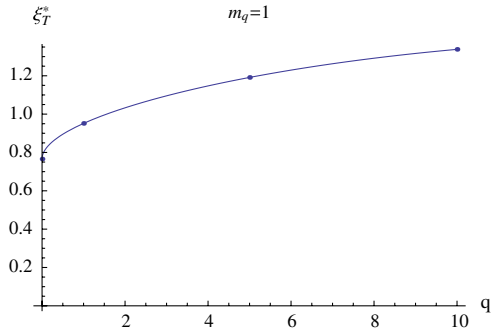

FIG. 4 (color online). q dependence of phase-transition temperature.

negative. Moreover, in Fig. 5(f), free energy of Minkowski embedding is always smaller than free energy of black-hole embedding. It means that in the $m_q \to 0$ limit, the value of chiral condensation does not vanish; see Fig. 6. This is a spontaneous breaking of a $U(1)$ symmetry which is an analogue of the chiral symmetry discussed [20,21]. Although the relevant symmetry is the rotation in the x^8, x^9 plane which is not a true chiral symmetry, one can develop the Gellman-Oakes-Renner relation [20,21], which is the purpose of having the chiral symmetry. Therefore, from now on, we call this chiral symmetry breaking and we call c the chiral condensation.

For a given temperature, the chiral symmetry is broken if q is large enough. The q dependence of the chiral-symmetry-restoring temperature is drawn in Fig. 7. When $q \to 0$, chiral-symmetry-restoring temperature goes to zero.

IV. CHIRAL SYMMETRY AT FINITE TEMPERATURE AND FINITE BARYON DENSITY

In this section, we discuss D7-brane embedding with finite density using the induced metric (2.6). Adding density corresponds to turning on the $U(1)$ gauge field $A_t(\rho)$ on the D7-brane. The DBI action of the D7-brane can be written

$$S_{D7} = -\tau_7 \int dtd\rho\rho^3 e^{\Phi/2}\omega_+^{3/2}\sqrt{e^{\Phi/2}\frac{\omega_-^2}{\omega_+}(1+\dot{y}^2) - \tilde{F}^2} := \int dtd\rho\, \mathcal{L}_{D7}, \tag{4.1}$$

where

$$\tau_7 = \mu_7 V_4 \Omega_3, \qquad \tilde{F} = 2\pi\alpha' F_{t\rho} \tag{4.2}$$

and dot denotes the derivative with respect to ρ. We used the $A_\rho = 0$ gauge. For a fixed-charge dynamics, we need the Legendre transformation of the Lagrangian, which we call "Hamiltonian":

$$\begin{aligned}\mathcal{H}_{D7} &= \tilde{F}\frac{\partial \mathcal{L}_{D7}}{\partial \tilde{F}} - \mathcal{L}_{D7} \\ &= \tau_7\sqrt{e^{\Phi}\frac{\omega_-^2}{\omega_+}(1+\dot{y}^2)}\sqrt{\hat{Q}^2 + \rho^6 e^{\Phi}\omega_+^3},\end{aligned} \tag{4.3}$$

where $\hat{Q} = Q/(2\pi\alpha'\tau_7)$, Q is the number of source charges. Notice that near the horizon, the last factor is dominated by the dilatonic term, and the whole action is reduced to the case of $Q = 0$. Therefore, the argument for

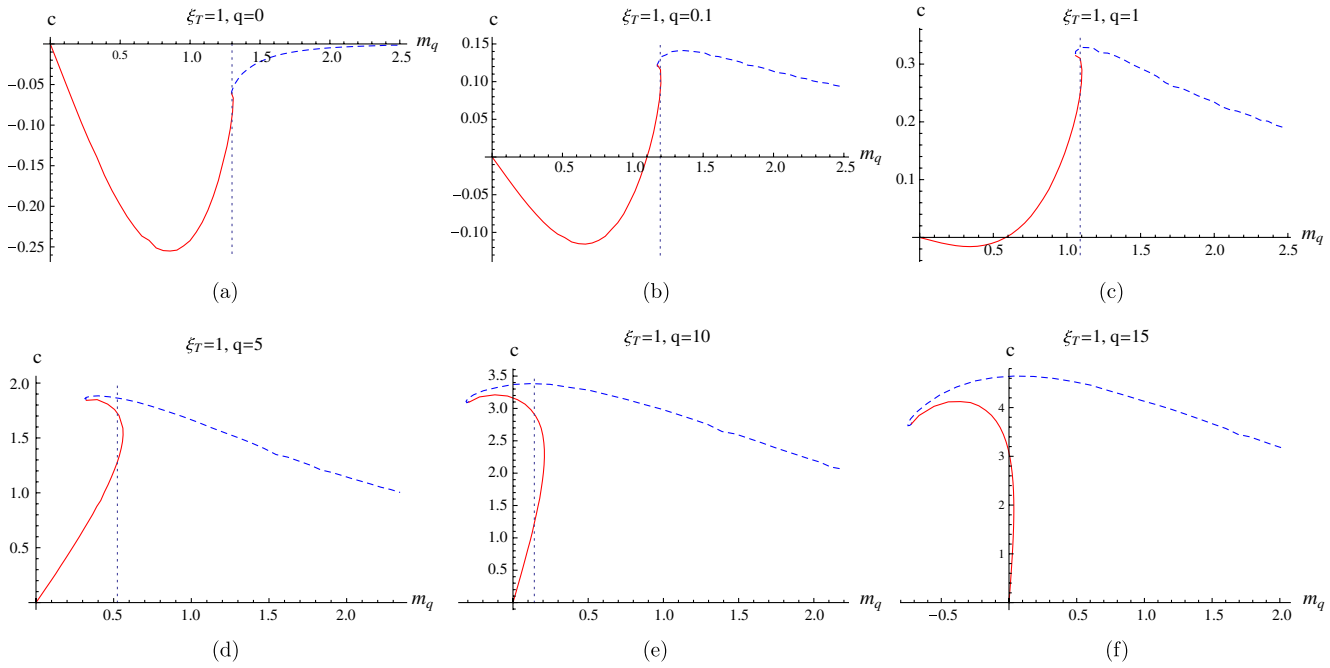

FIG. 5 (color online). m_q dependence of chiral condensation c for $\xi_T = 1$. The blue dashed line denotes chiral condensation for Minkowski embedding, and the red line denotes black hole embedding. The dotted line indicates phase transition between two embeddings.

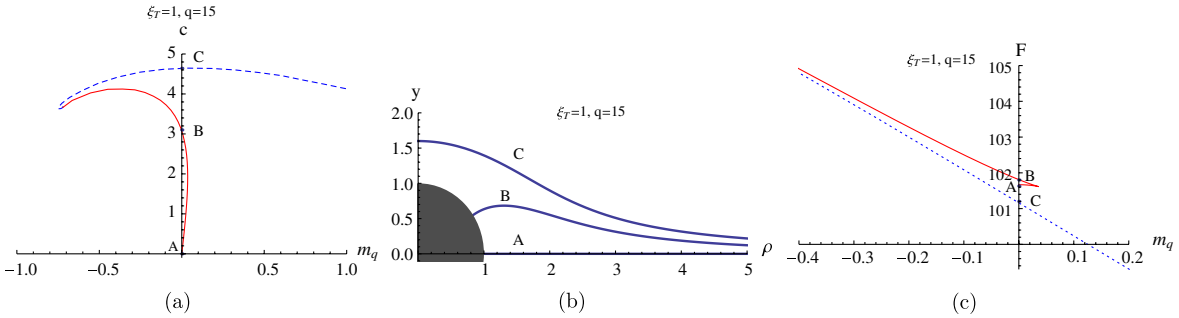

FIG. 6 (color online). (a) Fig. 5(f). A, B and C denote three solutions which give zero quark mass. (b) Probe-brane embeddings for each case. (c) Free energy as a function of quark mass. (c) Minkowski embedding has minimum energy.

the regularity near the horizon goes exactly the way of the previous section. We can get a numerical solution for the equation of motion provided we have proper boundary conditions. The stringy objects corresponding to the sources on the D7-brane are the end points of fundamental strings.

Unlike usual black-hole background, our background permits the presence of a baryon vertex. Therefore, there are two ways of attaching fundamental strings on the D7-brane. One is connecting D7 to the black-hole horizon, and the other is connecting it to the baryon vertices. Two configurations give different boundary conditions for the D7-brane dynamics. We need to examine which configuration has lower free energy.

A. Quark phase

One way to put point electric sources on the D7-brane is to add fundamental strings such that one end of the strings are on D7 and the other end on the black-hole horizon. It is equivalent to add a freely moving quark in boundary theory because the fundamental strings can move freely on both D7 and the horizon. We call it "quark" phase. Since the tension of the D7-brane is always smaller than that of the fundamental string [13], the D7-brane pulls down to the horizon.

Regularity at the black-hole horizon requires

$$\dot{y}(\rho_{\min}) = \tan\theta, \tag{4.4}$$

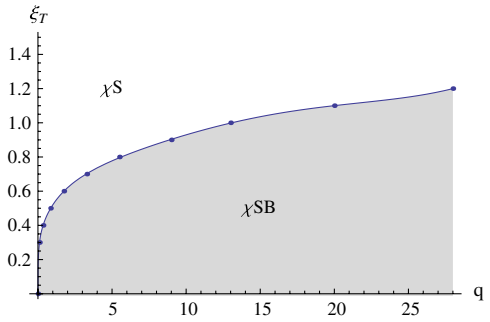

FIG. 7 (color online). q dependence of chiral-symmetry restoring temperature. χ^{SB} denotes chiral-symmetry breaking phase and χ^{S} denotes chiral-symmetry restored phase.

where θ is the polar angle of the position where the D7-brane touches the horizon. As discussed in the previous section, the presence of q gives repulsion on the probe D7-brane, and it affects its embedding. The q dependence of D7-brane embeddings are drawn in Fig. 8 for two different densities Q.

From the figure, we can see that as q increases, the repulsion effect on D7 also increases in small density $\hat{Q}$. However, if $\hat{Q}$ is not small, the brane embedding is less sensitive to q, as shown in Fig. 8(b). This is because the charge $\hat{Q}$ introduces a flux whose electric field energy increases the tension of the D7. That is, the stiffness due to the flux is dominating repulsion due to the q.

In the absence of q, the embedding solution which corresponds to $m_q = 0$ is uniquely determined to be the flat embedding, $y(\rho) = 0$, for which the value of chiral condensation is automatically zero. However, in the presence of q, there are two different embeddings for the given m_q. For $m_q = 0$, one is trivial with zero chiral condensation c, and the other has nonzero chiral condensation, as we can see in Fig. 9(a). The solution with nonzero c exists in the low-temperature and small-density region. In the large-density region, only $y = 0$ is the solution. Actually, we found that there is a phase transition between the two embeddings in certain temperature and density. The phase diagram is presented in Fig. 9(b). As q increases, the phase boundary expands toward a larger temperature and density region. See Fig. 10. This is natural since the chiral symmetry breaking is caused by the effect of gluon condensation q, as we have seen in Fig. 2.[1]

In Fig. 8, D7 embedding for nonzero m_q is drawn. In this case, behavior of the D7-brane embedding is similar to black-hole embedding with $q = 0$. Because of the nonzero value of $y(\infty) \sim m_q$, chiral symmetry is explicitly broken. However, it is known that there is first-order phase

[1]This phenomenon is very similar when we turn on the magnetic field on the probe brane [25] in the black D3-brane background. But in that case, the magnetic field cannot affect the background geometry, and the interpretation of magnetic field is also different.

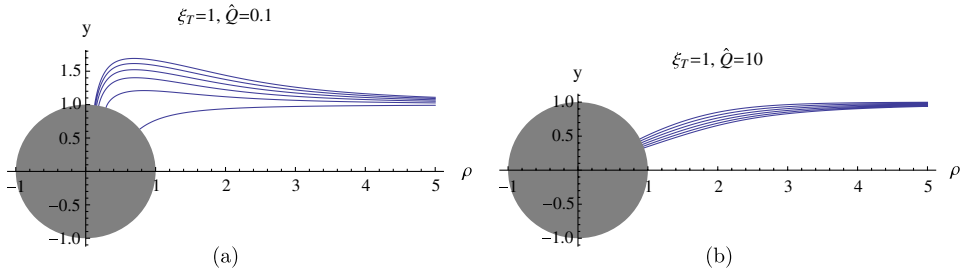

FIG. 8 (color online). D7-brane embeddings for $m_q = 1$ and $\xi_T = 1$ with $q = 0$, 2, 4, 6, 8, 10 from below for (a) $\hat{Q} = 0.1$, (b) $\hat{Q} = 10$.

transition in the black-hole background between two quark phases in the small-density region [12,13]. This phase transition line finishes at a certain density and temperature. At this point, the order of phase transition is second. As q increases, the phase boundary line moves upward in the (T, Q) plane. See Fig. 11.

There is an issue about thermodynamical instability around the first-order phase transition point in black-hole background [12,13]: chemical potential decreases as density increases; that is, $\partial\mu/\partial Q < 0$. But in the presence of q, this instability can be cured as we will discuss later.

B. Baryon phase

In this section, we study a baryon vertex in the D3/D-instanton background. Baryon vertex is originally proposed in Ref. [2]. Near-horizon geometry of a black D3-brane is $AdS_5 \times S^5$. If we wrap a spherical D5-brane on S^5, due to the Chern-Simons interaction between R-R fiveform field strength and D5-brane world volume, $U(1)$ gauge field is induced on the D5-brane world volume, and to cancel these fluxes, we need to put N_c fundamental strings on the D5-brane. In the asymptotic region, this object looks like a bound state of the N_c fundamental string or quark. We call this object "baryon vertex."

However, as discussed in Ref. [4], black-hole background does not allow compact D5-brane as a solution of the equation of motion of DBI action. Therefore, the quark phase is only physical in the finite temperature system. But, in the D3/D-instanton background, a compact D5-brane with N_c fundamental strings can be formed even in the black-hole background [14]. By connecting baryon vertex and the probe D7-brane [4], we can discuss thermodynamics of the finite density and temperature system.

To study properties of the baryon vertex, we rewrite the 10-dimensional metric (2.3):

$$ds^2 = e^{\Phi/2}\left[\frac{r^2}{R^2}(f(r)^2dt^2 + d\vec{x}^2) + R^2\left(\frac{d\xi^2}{\xi^2} + d\theta^2 + \sin^2\theta d\Omega_4^2\right)\right]. \quad (4.5)$$

We take (t, θ_α) as world volume coordinates of a compact D5-brane and turn on the $U(1)$ gauge field on it to have $F_{t\theta} \neq 0$. As the ansatz for the embedding of compact D5, we assume the $SO(5)$ symmetry so that the position of the D5-brane and gauge field depend only on θ, i.e. $\xi = \xi(\theta)$, $A_t = A_t(\theta)$, where θ measures the polar angle of S^5 from the north pole. The induced metric on the D5-brane is

$$ds_{D5}^2 = e^{\Phi/2}\left[\frac{r^2}{R^2}f^2dt^2 + R^2\left(\frac{\xi'^2}{\xi^2} + 1\right)d\theta^2 + R^2\sin^2\theta d\Omega_4^2\right], \quad (4.6)$$

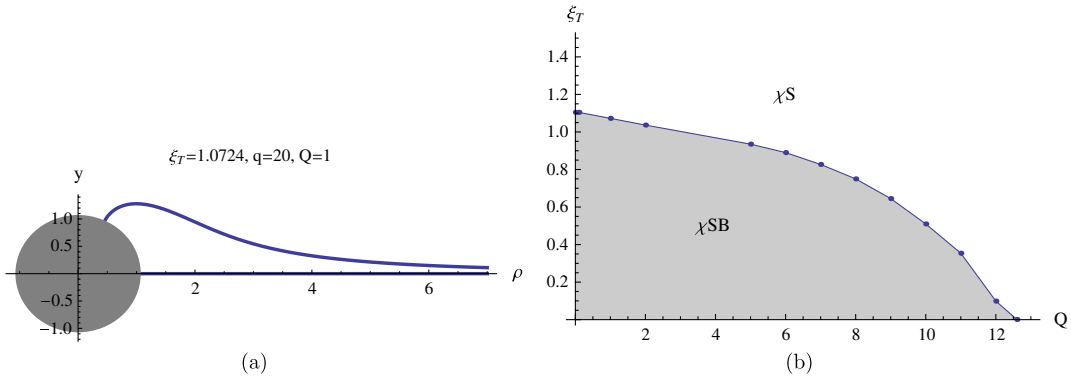

FIG. 9 (color online). (a) Two embedding solutions with the same temperature, density, and q. (b) Phase boundary between chiral-symmetry breaking and restored phases with $q = 20$.

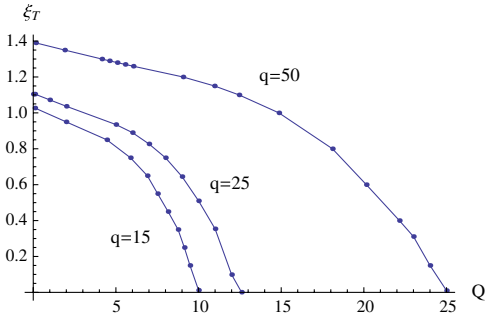

FIG. 10 (color online). Phase diagram of chiral-symmetry restoration within the quark phase for $q = 15$, 25 and 50.

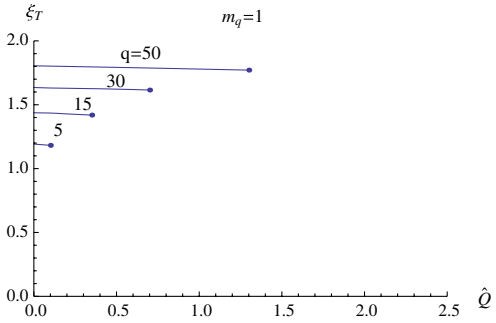

FIG. 11 (color online). q dependence of the phase transition between two quark phases for fixed $m_q = 1$. These phase transition lines end with the second-order phase-transition point.

where $\xi' = d\xi/d\theta$. The DBI action for a single D5-brane with N_c fundamental string can be written as

$$S_{D5} = -\mu_5 \int e^{-\Phi}\sqrt{-\det(g + 2\pi\alpha' F)} + \mu_5 \int A_{(1)} \wedge G_{(5)}$$
$$= \tau_5 \int dt d\theta \sin^4\theta e^{\Phi}\left[-\sqrt{e^{\Phi}\frac{\omega_-^2}{\omega_+}(\xi^2 + \xi'^2) - \tilde{F}^2} + 4\tilde{A}_t\right]$$
$$= \int dt d\theta \mathcal{L}_{D5}, \tag{4.7}$$

where

$$\tau_5 = \mu_5 \Omega_4 R^4 r_T, \qquad \tilde{F} = 2\pi\alpha' F_{t\theta}, \qquad \tilde{A}_t = 2\pi\alpha' A_t. \tag{4.8}$$

After solving the equation of motion for the gauge field and substituting it to the Lagrangian density, we can get the Hamiltonian density of the D5-brane,

$$\mathcal{H}_{D5} = \tau_5 \sqrt{\frac{e^{\Phi}}{2}\frac{\omega_-^2}{\omega_+}(\xi'^2 + \xi^2)}\sqrt{\hat{D}(\theta)^2 + \sin^8\theta}, \tag{4.9}$$

where

$$\hat{D}(\theta) = -\frac{3}{2}\theta + \frac{3}{2}\sin\theta\cos\theta + \sin^3\theta\cos\theta. \tag{4.10}$$

Here, we consider all fundamental strings are attached at the north pole. For more detail, see Appendix B.

The equation of motion for Eq. (4.9) depends on two parameters q, ξ_T and two initial conditions $\xi(\theta = 0) = \xi_0$, $\xi'(\theta = 0) = 0$. Here, we set $\theta = 0$ as the south pole of the D5-brane. For a given value of the expectation value of gluon condensation (q) and temperature (ξ_t), we can get a numerical solution in terms of ξ_0. The set of numerical solutions in the ξ plane is drawn in Fig. 12(a). In this figure, a cusp appears at $\theta = \pi$ where N_c fundamental strings are attached. But these closed D5-branes do not exist in the whole value of q and ξ_t. When the value of q decreases, the position of tip (we denote it to be ξ_c) increases, and in the $q \to 0$ limit, the tip of D5-brane goes to infinity (Fig. 12(b)). It is consistent with the fact that the usual Schwartzschild black-hole background does not allow a baryon vertex. We also check that the baryon-vertex solution does not exist at high temperature.

As we discussed in Ref. [4], we can add a D7-brane at the tip of the D5-brane with the force-balance condition [26],

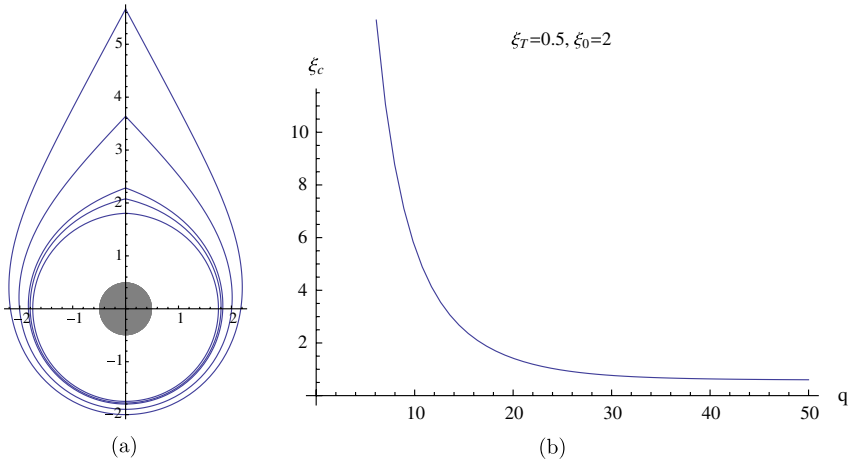

FIG. 12 (color online). (a) ξ_0 dependence of D5-brane embeddings with $q = 10$, $\xi_T = 0.5$. The gray disk denotes black hole. (b) q dependence of the tip of the D5-brane (ξ_c).

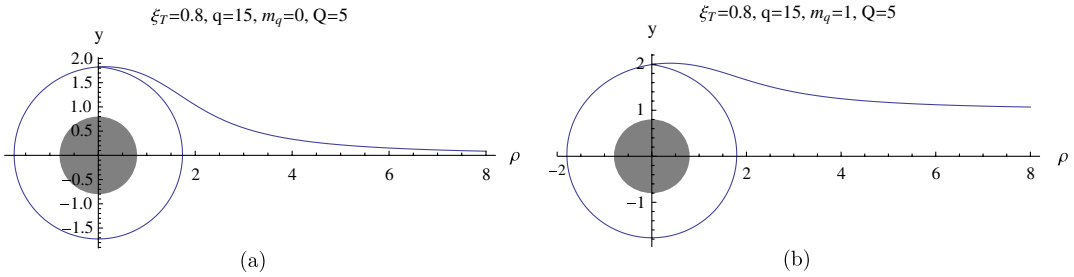

FIG. 13 (color online). D7-brane embeddings for $\xi_T = 0.8$, $\tilde{Q} = 5$ with (a) $m_q = 0$ (b) $m_q = 1$.

$$y'(\rho = 0) = \frac{\xi_c'}{\xi_c}, \tag{4.11}$$

where ξ_c and ξ_c' denote the position and slop of the D5-brane at $\theta = \pi$. For details, see Appendix C. The full configurations of D7/D5-brane embeddings with a certain value of q and density are drawn in Fig. 13. We call this phase "baryon phase" because in this phase, the physical object is the baryon vertex. From this figure, we can see that in the presence of the baryon vertex, the slope of the probe brane in the asymptotic region is always nonzero. It means that in the baryon phase, chiral symmetry is always broken. We found that the embedding corresponding to the baryon phase does not exist at high temperature.

V. PHASE TRANSITION

As we discussed in the previous section, two kinds of embeddings can exist in finite temperature. They correspond to two phases: black-hole embedding corresponds to the quark phase, and Minkowski embedding corresponds to the baryon phase. The quark phase can exist in a whole temperature region, while the baryon phase can exist only at the low-temperature region. In our model, the baryon phase exists if the temperature is low enough, regardless of how high the density is. However, in low temperature, the quark phase is also possible. To determine which is the physical phase, we need to compare the free energies of two systems. There are two ensembles we can choose, one is the canonical ensemble where density is a control parameter. In the canonical ensemble, we can determine the physical phase by comparing free energy. Since we need to determine the configuration in a fixed value of the charge, we need the Legendre-transformed action which we call Hamiltonian, although it is not the time-translation generator. The other one is the grand canonical ensemble where chemical potential is a control parameter. In this case, we have to calculate grand potential which is a value of the DBI action.

A. Canonical ensemble

To determine the physical solution in a canonical ensemble, we have to compare free energies of two phases. Free energy of the quark phase is given by integrating Hamiltonian (4.3) density for the embeddings,

$$\mathcal{F}_{\text{quark}}(\hat{Q}) = \tau_7 \int_{\rho_{\min}}^{\infty} d\rho \hat{\mathcal{H}}_{D7}(\hat{Q})|_{\text{quark phase}}, \tag{5.1}$$

where $\hat{\mathcal{H}}_{D7} = \mathcal{H}_{D7}/\tau_7$ (we introduce it for convenience). Here, we regularized free energy by subtracting energy of a flat D7-brane.

On the other hand, the baryon phase needs a compact D5-brane, called the baryon vertex operator. Since each D5 should have N_c quarks, their number is related to the quark number by $N_B = Q/N_c$. The total free energy in baryon phase can be obtained by adding energy of the D5-brane to that of the D7-brane:

$$\begin{aligned}\mathcal{F}_{\text{baryon}}(\hat{Q}) &= \tau_7 \int d\rho \hat{\mathcal{H}}_{D7}(Q)|_{\text{baryon phase}} \\ &\quad + \frac{Q}{N_C}\tau_5 \int d\theta \hat{\mathcal{H}}_{D5} \\ &= \tau_7 \Big[\int d\rho \hat{\mathcal{H}}_{D7}(\hat{Q})|_{\text{baryon phase}} \\ &\quad + \frac{2}{3\pi}\hat{Q} \int d\theta \hat{\mathcal{H}}_{D5} \Big].\end{aligned} \tag{5.2}$$

By comparing the value of Eqs. (5.1) and (5.2), we can determine which phase is physically favored. As we discussed in the previous section, there are two phases in the quark phase, which is true also in the massless quark case. One is the quark phase with broken chiral symmetry, and the other one is a phase with chiral symmetry restored. The density dependences of free energy in the massless quark case are drawn in Fig. 14. In the figure, we plotted $\tilde{F}$ which is defined as $\tilde{F} = F - \alpha(T)Q$ to visualize the difference of the free energies of different phases. One should notice that all the free energies monotonically increase as functions of density, although the figure does not show it due to the subtraction of $\alpha(T)Q$.

At low temperature, the free energy of the baryon phase is always lower than that of the quark phase for all density regions, see Fig. 14(a). It means that the baryon phase is physical at low temperature. As temperature increases, the free-energy lines change drastically; see Fig. 14(b). At temperature $\xi_t = 0.16$, the free energy of the baryon phase is lowest in the low density region. As density increase, there is phase transition between the baryon phase and quark phase with broken chiral symmetry (first vertical line in Fig. 14(b)). After the baryon-to-quark phase

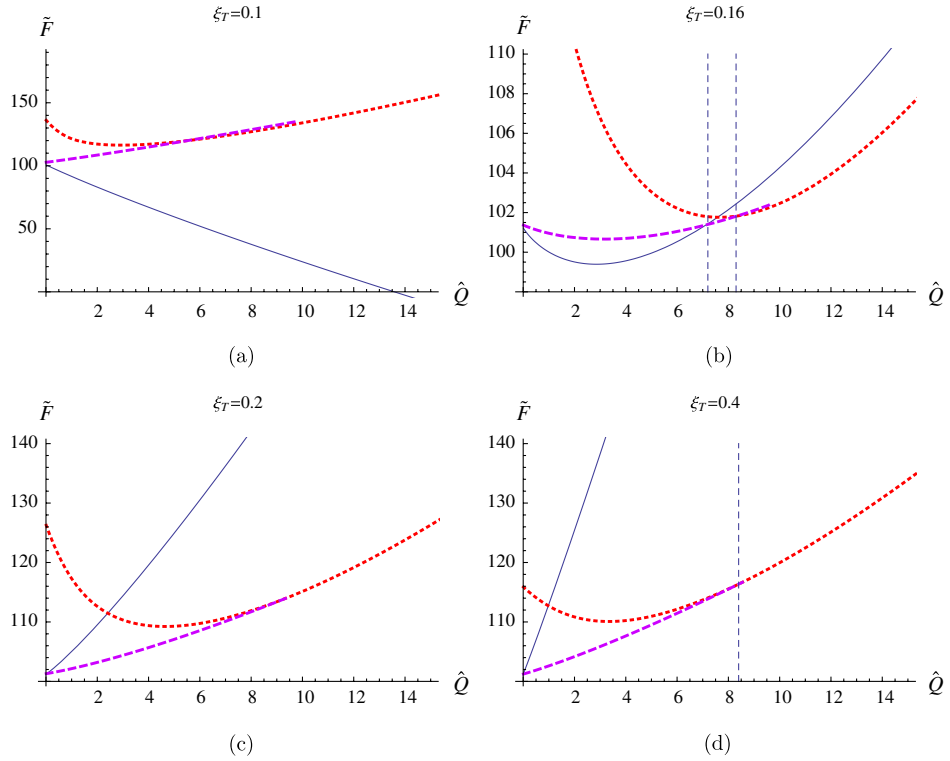

FIG. 14 (color online). Density dependence of free energy for the massless quark case with $q = 15$. To visualize the difference of free energy, we plotted $\tilde{F}$ which is defined as $\tilde{F} = F - \alpha(T)Q$ for some $\alpha(T)$. The solid line is for the baryon phase, red dotted line is for the chiral-symmetry restored quark phase, and the dashed purple line is for the quark phase with chiral symmetry broken. The vertical dotted line denotes the phase transition point.

transition, there is another phase transition between quark phases: from broken to restored chiral-symmetry quark phase. At higher temperature, the free energy of the quark phase is always smaller than that of the baryon phase. But there is a phase transition from chiral-symmetry broken phase to chiral-symmetry restored phase at a certain density. See Figs. 14(c) and 14(d). The chiral phase transition between two quark phases coincides with the result of the previous section, Fig. 10. Of course, at high enough temperature, the chiral-symmetry restored quark phase is the only physical phase. These are summarized in the phase diagram drawn in Fig. 15.

This phase diagram has a rich structure. At low temperature, the baryon phase is always a physical one in all density regions. And chiral symmetry is always broken in this phase. However, as we increase temperature, phase transition appears differently depending on density. At low density, as temperature increases, the baryon phase changes into the quark phase, but chiral symmetry is still broken. If we increase temperature more, then there is chiral-symmetry restoration transition in the quark phase. On the other hand, at high density, as we increase temperature, the baryon/quark phase transition and chiral phase transition appear at the same time.

We find that the baryon/quark phase transition temperature decreases as density increases. However, the decreasing rate is too slow so that phase-transition temperature looks like a constant in the figure. The value of q also affects phase transition. As q increases, both phase boundaries move up to a larger temperature and larger density region maintaining the overall shape. See Fig. 15(b). Notice that our phase diagram is very similar to the ones for the Sakai-Sugimoto model studied in Ref. [27], where the baryon phase should be replaced by the soliton geometry. Notice that in our model, there is no Hawking-Page transition since there is no scale other than the temperature and the dilaton contribution is precisely canceled by that of the axion. Our baryon phase is still in the black-hole geometry; therefore, the dynamic origin is very different.

In the case of $m_q \neq 0$, chiral symmetry is explicitly broken so that we might expect that there is only the baryon/quark phase transition. However, as we discussed in the previous section, there is another phase transition in the quark phase. Look at the short line at the upper-left region of the phase diagram in Fig. 16. It is for $m_q = 1$.

As we decrease the quark mass, the end point of the phase boundary extends to a higher density and lower temperature region so that when $m_q \to 0$, we recover the phase diagram drawn in Fig. 15. Actually, the line becomes long very fast when m_q gets to the near-zero value. Contrarily, for $q = 0$, the line for the transition from

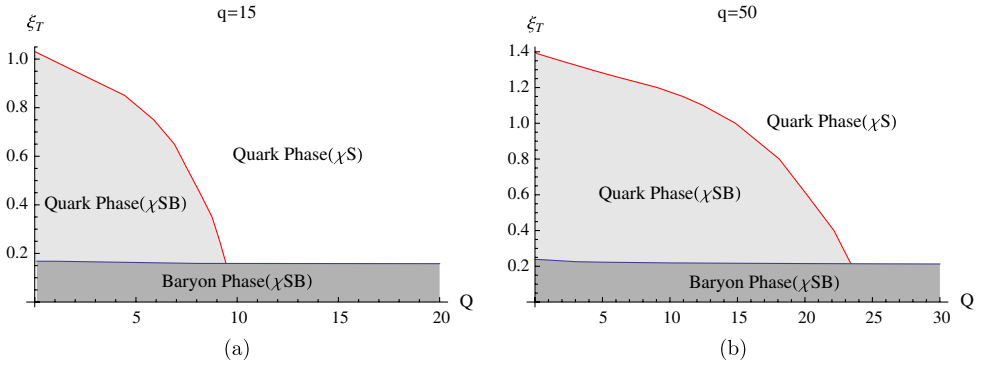

FIG. 15 (color online). Density dependence of phase transition temperature between the quark phase and baryon phase (a) with $q = 15$, (b) with $q = 50$.

black-hole embedding to another black-hole embedding exists only in a very small density region, and it disappears when m_q goes to zero. Therefore, this is a very characteristic feature caused by the gluon condensation q.

B. Relation between chemical potential and density

Equations of state which are the relations between thermodynamically conjugate variables like chemical potential/density, quark mass/chiral condensation, etc., play an important role to understand phase structure. In this section, we will discuss the equation of state describing the relation between chemical potential and density. Thermodynamically chemical potential is defined as the derivative of free energy with respect to density,

$$\mu = \frac{\partial \mathcal{F}}{\partial Q}. \tag{5.3}$$

In the quark phase, we can get

$$\begin{aligned}\mu_{\text{quark}} &= \frac{\partial \mathcal{F}_{\text{quark}}}{\partial Q} = \frac{1}{2\pi\alpha'}\int_{\rho_{\text{min}}}^{\infty}\frac{\partial \hat{\mathcal{H}}_{D7}}{\partial \hat{Q}} \\ &= \int_{\rho_{\text{min}}}^{\infty} d\rho\, \partial_\rho A_t = A_t(\infty) - A_t(\rho_{\text{min}}).\end{aligned} \tag{5.4}$$

In this case, $A_t(\rho_{\text{min}}) = 0$ because ρ_{min} is the black-hole horizon. It is consistent with the usual definition of chemical potential (tale of A_t field) from AdS/CFT correspondence. On the other hand, the free energy of the baryon phase contains mass of the baryon vertex, and chemical potential should have mass of the source.

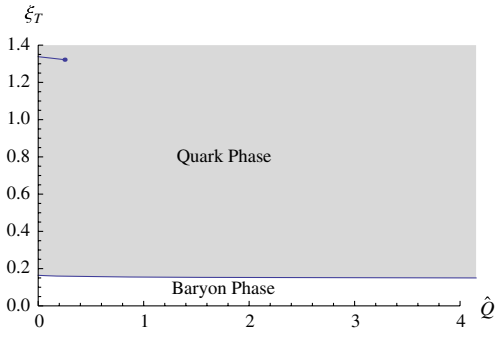

FIG. 16 (color online). Density dependence of phase-transition temperature between the quark phase and baryon phase for $m_q = 1$ and $q = 20$.

$$\begin{aligned}\mu_{\text{baryon}} &= \frac{\partial \mathcal{F}_{\text{baryon}}}{\partial Q} \\ &= \frac{1}{2\pi\alpha'}\int_{\rho_{\text{min}}}^{\infty}\frac{\partial \hat{\mathcal{H}}_{D7}}{\partial \hat{Q}} + \frac{1}{2\pi\alpha'}\frac{2}{3\pi}\int d\theta \hat{\mathcal{H}}_{D5} \\ &= A_t(\infty) - A_t(\rho_{\text{min}}) + \frac{1}{N_c}\int d\theta \mathcal{H}_{D5}.\end{aligned} \tag{5.5}$$

Eq. (5.5) is the baryon mass divided by N_c, which is the constituent quark mass. Therefore, the chemical potential contains mass of the source. In the quark phase, the source is the fundamental strings. For the black-hole embedding, the D7-brane touches the black-hole horizon, and the fundamental strings are replaced by deformation of the D7-brane. Therefore, the energy of fundamental strings is contained in that of the D7-brane. That is why there is no source term [the analogue of the last term in the Eq. (5.5)] in the chemical potential of the quark phase. The density dependences of chemical potential for $m_q = 0$ embedding are drawn in Fig. 17. We can see that chemical potentials monotonically increase as density increases for any phases. Therefore, there is no thermodynamical instability in the $m_q = 0$ case.

The free energy and chemical potential with finite quark mass as functions of density are drawn in Fig. 18. Figure 18(a) shows density dependence of free energy at finite temperature with $q = 50$ and $m_q = 1$. At a certain density, there is phase transition in the quark phase. In usual AdS Schwartzschild background without q, there is a thermodynamical instability associated with the negative slope branch of the μ-Q diagram. But in Fig. 18(b), we can see that chemical potential increases at low density, and phase transition happens before chemical potential begin to decrease. Therefore, chemical potential for the physical state always increases monotonically as density increases

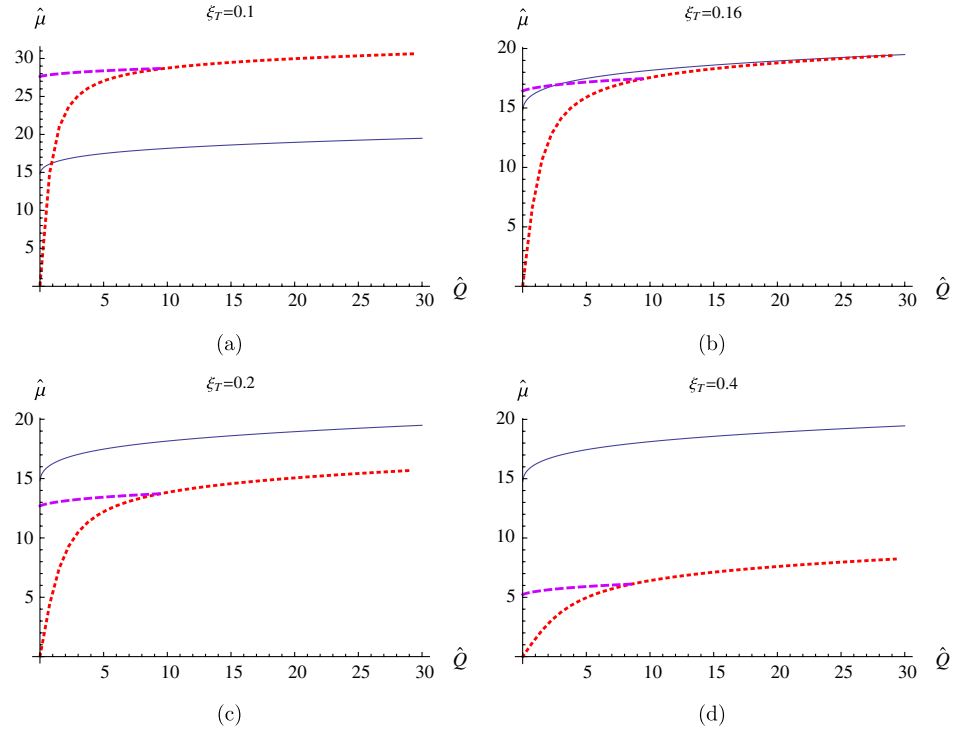

FIG. 17 (color online). Density dependence of the chemical potential for $m_q = 0$. The red dotted line denotes chemical potential for the quark phase with chiral symmetry, and the purple dashed line is for the quark phase with broken chiral symmetry. The solid line denotes the baryon phase.

$(\partial\mu/\partial Q > 0)$; hence, there is no thermodynamical instability.

As temperature decreases, both quark phase and baryon phase exist, and the shape of chemical potential is monotonic as a function of the density in both phases which is similar to Fig. 17.

C. Grand canonical ensemble

In this section, we will discuss the system with grand canonical ensemble. Grand potential is thermodynamically defined as

$$\Omega = \mathcal{F} - \mu Q. \tag{5.6}$$

From the definition of Hamiltonian density and number density, grand potential for the quark phase can be written as

$$\begin{aligned}\Omega_{\text{quark}} &= \mathcal{F}_{\text{quark}} - \mu_{\text{quark}} Q \\ &= \int \tilde{F} \frac{\partial \mathcal{L}_{D7}}{\partial \tilde{F}}\Big|_{\text{quark phase}} - \int \mathcal{L}_{D7}|_{\text{quark phase}} - \int \tilde{F}\tilde{Q} \\ &= -\int \mathcal{L}_{D7}|_{\text{quark phase}}.\end{aligned} \tag{5.7}$$

The last term in Eq. (5.7) is nothing but the value of on-shell DBI action for the black-hole phase. It is obvious because "Hamiltonian density" is defined by Legendre

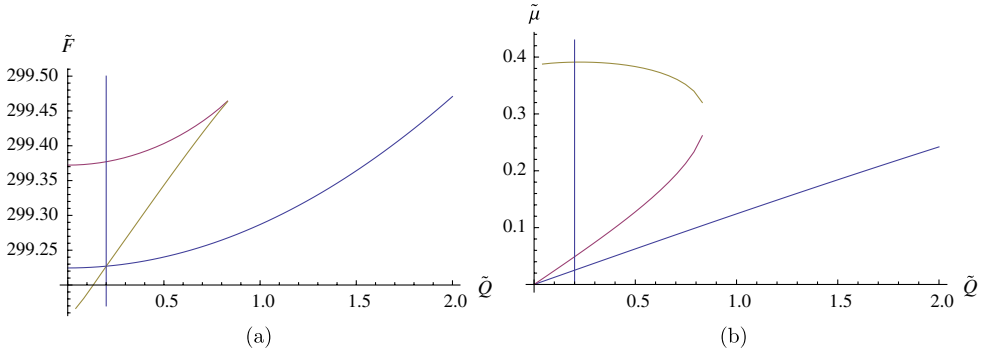

FIG. 18 (color online). (a) Free energy as a function of density in certain temperature for $m_q = 1$. (b) Density dependence of the chemical potential, $\tilde{\mu} = 2\pi\alpha'\mu$. In both figures, $\xi_T = 1.3$, $q = 50$.

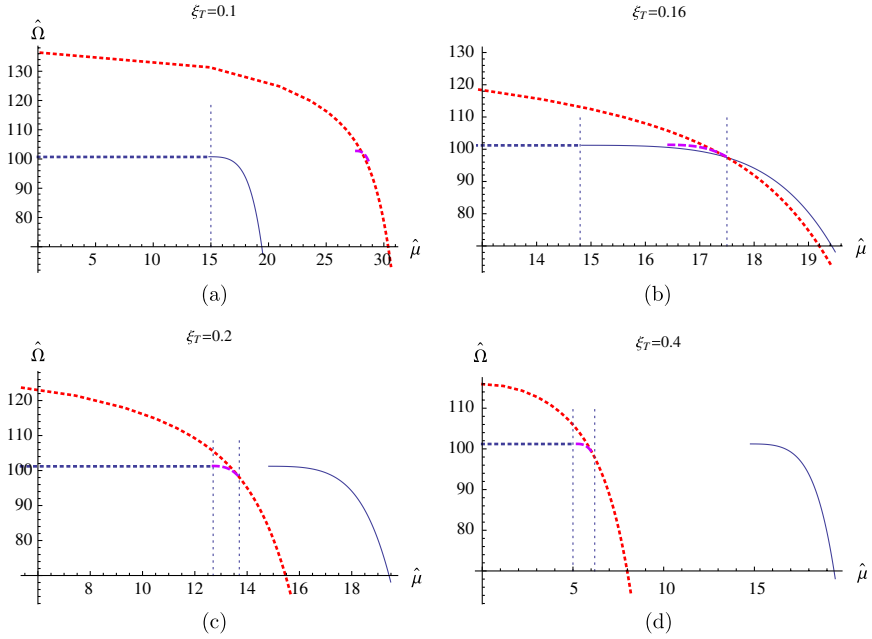

FIG. 19 (color online). Chemical potential dependence of grand potential ($m_q = 0$ and $q = 15$). The red dotted line denotes grand potential for the chiral-symmetry restored quark phase. The purple dashed line is for the quark phase without chiral symmetry, and the solid line is for the baryon phase

transformation of DBI action. Grand potential for the baryon phase becomes

$$\begin{aligned}\Omega_{\text{baryon}} &= \mathcal{F}_{\text{baryon}} - \mu_{\text{baryon}} Q \\ &= \int \mathcal{H}_{D7}|_{\text{baryon phase}} + \frac{Q}{N_c}\int \mathcal{H}_{D5} \\ &\quad - \left(\int \tilde{F}\,\tilde{Q} + \frac{Q}{N_c}\int \mathcal{H}_{D5}\right) \\ &= -\int \mathcal{L}_{D7}|_{\text{baryon phase}}. \end{aligned} \tag{5.8}$$

We can see that the energy of source in free energy canceled by one in chemical potential, finial form of grand potential is the value of DBI action of the D7-brane for the baryon phase. Notice that the D5 part does not contribute to grand potential.

In the massless quark case ($m_q = 0$), the grand potentials of the quark and baryon phases are drawn in Fig. 19. In each case of that figure, chemical potential starts from a nonzero value, as one can see in Fig. 17. It implies that if the chemical potential is not large enough compared to the energy of particle, no particle can be created. Therefore, the system remains as a vacuum until chemical potential reaches to the energy of the particle in the system. Therefore, the value of the chemical potential should be identified as the constituent quark mass. Naturally, the difference in the chemical potential in the baryon phase and that in the realized quark phase (between the two quark phases) can be identified as the binding energy. The density dependence of the quark mass is plotted in Fig. 19. The phase transition point can be identified precisely as the point where the binding energy is 0. This point is of course the point where baryons melt. The melting point in the temperature-density plane is nothing but our phase diagram.

From Fig. 19, one can easily read off the critical chemical potential value points as one increases the temperature.

In the case of finite quark mass, chiral symmetry is always broken similarly to the canonical ensemble. We have only two phases: the baryon phase and quark phase. However, we find that the density dependence of chemical potential and the chemical potential dependence of grand potential behave similarly to the massless case except in the absence of chiral phase transition. The phase structure based on the above discussion is drawn in Fig. 20. Similar to the phase diagram in the canonical ensemble, the temperature of the phase transition between the quark and baryon phase is almost constant. We also find the transition in the quark phase in the small density region, but this line is not shown in this diagram.

D. Chiral condensation

One of the most important observables in QCD is the chiral condensation and its density dependence. It measures the dynamical mechanism for creating the mass of the hadrons. Figure 21 shows the density dependence of the chiral condensation. In the baryon phase, chiral symmetry is always broken, and there is a quark phase where chiral symmetry is broken. Our result shows that chiral condensation is increasing in the baryon phase and decreasing in the relevant quark phase.

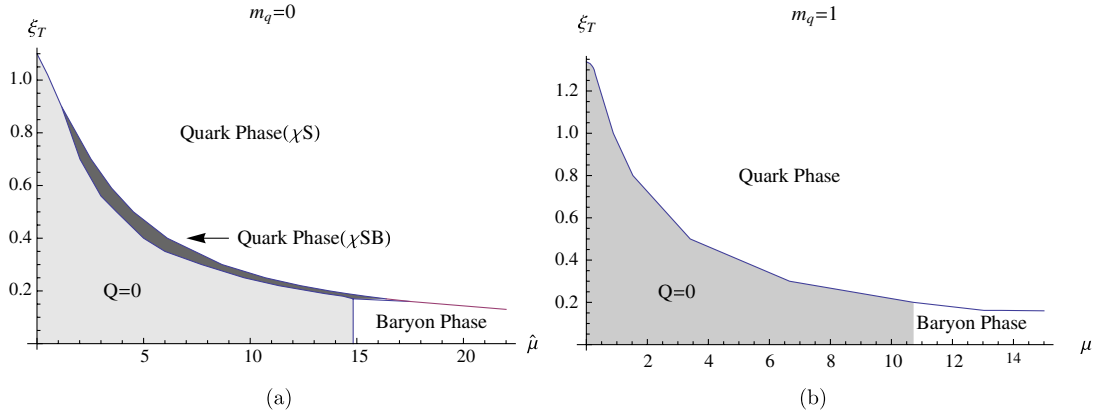

FIG. 20 (color online). Phase diagrams in grand canonical ensemble with (a) $m_q = 0$, (b) $m_q = 1$.

VI. SUMMARY AND DISCUSSION

In this paper, we study the phase structure of a holographic QCD based on a D3/D-instanton background. The phase transition here is for confinement/deconfinement of quarks, not the gluons. While the Hawking-Page transition in usual AdS/CFT correspondence describes the dynamics of the gluon, the confinement/deconfinement phase transition of quarks is determined from the interaction between the geometry and the compact brane dynamics. Namely, it is a question of existence of the baryon vertex. The D3/D-instanton background has quasiconfining nature as defined in the introduction. In the zero-quark-mass case, there is a chiral transition in the quark phase. The number of D-instanton, identified as the expectation value of gluon condensation, played an essential role in breaking the chiral symmetry. The phase boundary depends on the value of q.

A few remarks are in order:

The first one is on the assumption that there is no Hawking-Page transition. The main reason is that the geometric transition should be discussed in the Einstein frame, where dilaton action is cancelled by that of the axion; therefore, we cannot find any effect of the dilaton condensation scale in the bulk free-energy level. In addition, it is completely the same as the D3-brane without

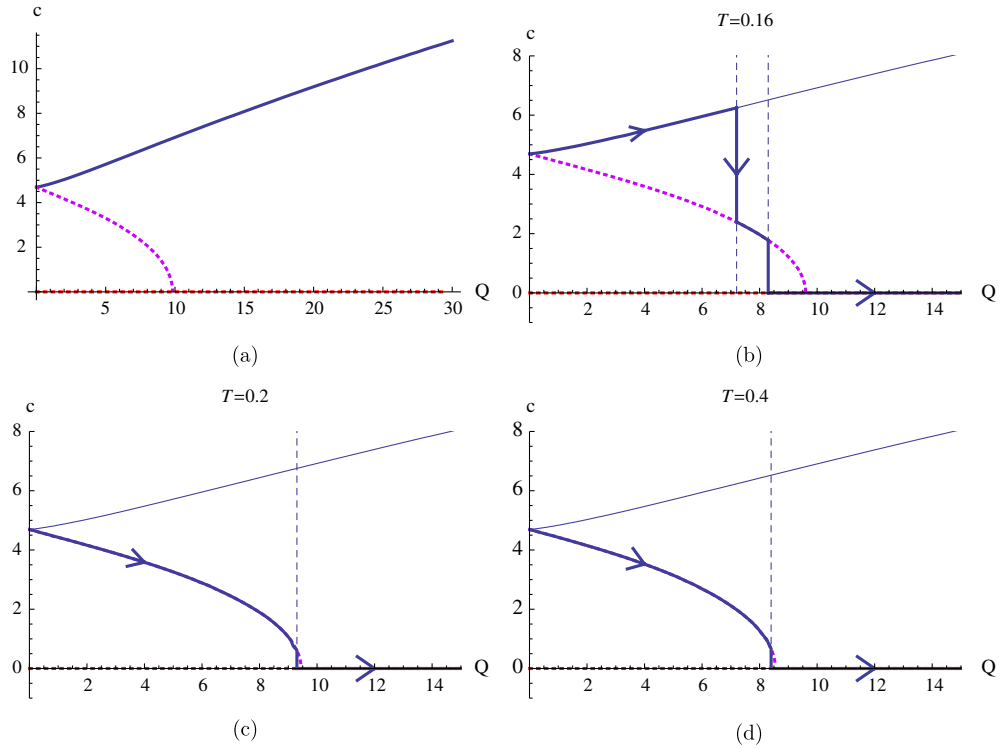

FIG. 21 (color online). Density dependence of the value of chiral condensation $\langle\bar{q}q\rangle$ for the massless quark case with $q = 15$. The thick line indicates the physical phase from free energy, and there is phase transition along the vertical dashed line.

D-instanton. However, all the probe D-brane dynamics is affected by the presence of the dilaton factor. That is why we get a nontrivial result. This is an interesting and subtle point, and in the main sections, we just assumed that there is no Hawking-Page transition.

The second one is about the role of the Chern-Simons term. In Ref. [7], the authors introduced the Chern-Simons term such that it cancels out the dilaton effect of the brane-embedding dynamics. However, we could not find a solution with such behavior. We found that the Chern-Simons term is a total derivative so that it can contribute to the charge but not to the equation of motion. This allows us the nontrivial effect of the gluon condensation on the embedding of the D7-brane as well as on that of D5.

The third one is that due to the probe nature of the embedding dynamics, our calculation is not trusted in the extreme high-density regime. One needs to take care of the backreaction of probe branes to the geometry.

The fourth is the Euclidean nature and duality in such a background. For the Euclidean configuration, there is no state/geometry correspondence. However, gauge-gravity duality is still there. The correspondence of the D-instanton in type IIB and Yang-Mills theory instantons was discussed in Ref. [28] as well as many other papers. The relation of AdS/CFT and multi-instanton gauge theory is considered in well-known works of Dorey *et al.* [29]. So, the gauge-theory dual of the uniform distribution of such a D-instanton is not hard to imagine, and it should be the Yang-Mills theory with uniform distribution of instanton charge.

The fifth is the infrared singularity. The background has the IR singularity since the dilaton factor has log singularity at the horizon. Usually, one needs to prevent any D-brane probe to approach such a singular region. Also, this makes the bulk action divergent, and we would need an IR cut off. However, in our background, both the bulk gravity action as well as the DBI action are regular at the horizon. There is no divergence. There are reasons for this: i) The finite-temperature version has a regular horizon, and the essential singularity is hidden in the horizon. ii) The finiteness of the bulk action is partly due to the supersymmetric construction of the action and the ansatz Eq. (3.1) by which the action of dilaton is cancelled precisely by that of the axion. iii) The finiteness of the probe-brane action is due to the detailed structure of DBI action. Looking at Eq. (4.7), the log divergence of dilaton factor e^{Φ} is cancelled by the presence of the ω_- factor, which is canceled by the zero ω_-. The thermodynamics is based on the calculation of the DBI action for the actual configuration of the probe brane. Speaking more physically, the background acts net repulsive force to the D-brane which performs a dynamic censorship and gives finite values of DBI action.

In the background with $q = 0$, the meson spectral function does not have this interesting feature. But due to the repulsive nature of the force acting on the probe brane, there is some reason to expect nontrivial spectral behavior in this case. It would be very interesting to calculate the meson spectrum in the chiral-symmetry broken quark phase.

ACKNOWLEDGMENTS

This work was supported by the National Research Foundation of Korea (NRF) grant funded by the Korea government (MEST) through the Center for Quantum Spacetime (CQUeST) of Sogang University with Grant No. 2005-0049409. The work of Y. S. and S. J. S. was supported by Mid-career Researcher Program through NRF Grant No. 2010-0008456. The work of M. K. was supported in part by KRF-2007-313- C00150, WCU Grant No. R32-2008-000-101300.

APPENDIX A: CHERN-SIMONS TERM

On a probe D7-brane, the 8-form field, which is the Hodge dual of the axion, can interact with the D7-brane world volume through the CS term. This coupling does not affect the equation of motion. Here, we give an explicit check for this in the zero-temperature case.

In the limit $T \to 0$, Eq. (2.2) becomes

$$\begin{aligned} ds &= e^{\Phi/2}\left\{\frac{r^2}{R^2}(-dt^2 + d\vec{x}^2) + \frac{R^2}{r^2}(dr^2 + r^2 d\Omega_5^2)\right\}, \\ e^{\Phi} &= 1 + \frac{q}{r^4}, \qquad \chi = -e^{-\Phi} + \chi_\infty. \end{aligned} \tag{A1}$$

We are interested in the interaction between the dual field of the axion and probe D7-brane. We change the metric into the direction along and perpendicular to the D7-brane,

$$\begin{aligned} ds = e^{\Phi/2}\Big\{&\frac{r^2}{R^2}(-dt^2 + d\vec{x}^2) + \frac{R^2}{r^2}(d\rho^2 + \rho^2 d\Omega_3^2 \\ &+ dy^2 + y^2 d\phi^2)\Big\}, \end{aligned} \tag{A2}$$

where $r^2 = \rho^2 + y^2$. To get the dual field, we introduce vierbein

$$\begin{aligned} e^{\tilde{t}} &= e^{\Phi/4}\frac{r}{R}\mathrm{d}t, \qquad e^{\tilde{x}_i} = e^{\Phi/4}\frac{r}{R}\mathrm{d}x_i, \\ e^{\tilde{\rho}} &= e^{\Phi/4}\frac{R}{r}\mathrm{d}\rho, \qquad e^{\tilde{\Omega}_3} = e^{\Phi/4}\frac{R}{r}\rho\mathrm{d}\Omega_3, \\ e^{\tilde{y}} &= e^{\Phi/4}\frac{R}{r}\mathrm{d}y, \qquad e^{\tilde{\phi}} = e^{\Phi/4}\frac{R}{r}y\mathrm{d}\phi, \end{aligned} \tag{A3}$$

where tilde denotes a flat index. The field strength for the axion field is

$$\begin{aligned} F_{(1)} &= \mathrm{d}\chi = \frac{\partial\chi}{\partial r}\mathrm{d}r = e^{-\Phi}\frac{\partial\Phi}{\partial\rho}\mathrm{d}\rho + e^{-\Phi}\frac{\partial\Phi}{\partial y}\mathrm{d}y \\ &= e^{-5\Phi/4}\frac{\partial\Phi}{\partial\rho}\frac{r}{R}e^{\tilde{\rho}} + e^{-5\Phi/4}\frac{\partial\Phi}{\partial y}\frac{r}{R}e^{\tilde{y}}. \end{aligned} \tag{A4}$$

The Hodge dual of this field strength is

$$F_{(9)} = \frac{1}{9!}e^{-5\Phi/4}\frac{\partial\Phi}{\partial\rho}\frac{r}{R}\epsilon^{\tilde{\rho}}_{\tilde{t}\tilde{x}_i\tilde{\Omega}_3\tilde{y}\tilde{\phi}}e^{\tilde{t}}\wedge e^{\tilde{x}_i}\wedge e^{\tilde{\Omega}_3}\wedge e^{\tilde{y}}\wedge e^{\tilde{\phi}} + \frac{1}{9!}e^{-5\Phi/4}\frac{\partial\Phi}{\partial y}\frac{r}{R}\epsilon^{\tilde{y}}_{\tilde{t}\tilde{x}_i\tilde{\Omega}_3\tilde{\rho}\tilde{\phi}}e^{\tilde{t}}\wedge e^{\tilde{x}_i}\wedge e^{\tilde{\rho}}\wedge e^{\tilde{\Omega}_3}\wedge e^{\tilde{\phi}}$$
$$= e^{\Phi}\frac{\partial\Phi}{\partial\rho}\rho^3 y\mathrm{d}t\wedge\mathrm{d}\vec{x}\wedge\mathrm{d}\Omega_3\wedge\mathrm{d}y\wedge\mathrm{d}\phi - e^{\Phi}\frac{\partial\Phi}{\partial y}\rho^3 y\mathrm{d}t\wedge\mathrm{d}\vec{x}\wedge\mathrm{d}\Omega_3\wedge\mathrm{d}\rho\wedge\mathrm{d}\phi$$
$$= \frac{\partial e^{\Phi}}{\partial\rho}\rho^3 y\mathrm{d}t\wedge\mathrm{d}\vec{x}\wedge\mathrm{d}\Omega_3\wedge\mathrm{d}y\wedge\mathrm{d}\phi - \frac{\partial e^{\Phi}}{\partial y}\rho^3 y\mathrm{d}t\wedge\mathrm{d}\vec{x}\wedge\mathrm{d}\Omega_3\wedge\mathrm{d}\rho\wedge\mathrm{d}\phi, \tag{A5}$$

where we are using the convention

$$\epsilon_{\tilde{t}\tilde{x}_i\tilde{\rho}\tilde{\Omega}_3\tilde{y}\tilde{\phi}} = +1. \tag{A6}$$

By substituting e^{Φ}, we get

$$F_{(9)} = -\frac{4q\rho^4 y}{(\rho^2+y^2)^3}\mathrm{d}t\wedge\mathrm{d}\vec{x}\wedge\mathrm{d}\Omega_3\wedge\mathrm{d}y\wedge\mathrm{d}\phi + \frac{4q\rho^3 y^2}{(\rho^2+y^2)^3}\mathrm{d}t\wedge\mathrm{d}\vec{x}\wedge\mathrm{d}\Omega_3\wedge\mathrm{d}\rho\wedge\mathrm{d}\phi. \tag{A7}$$

Now, we want to get the 8-form potential such that

$$F_{(9)} = \mathrm{d}C_{(8)}. \tag{A8}$$

Assuming

$$C_{(8)} = f(\rho, y, \phi)\mathrm{d}t\wedge\mathrm{d}\vec{x}\wedge\mathrm{d}\Omega_3\wedge\mathrm{d}y + g(\rho, y, \phi)\mathrm{d}t\wedge\mathrm{d}\vec{x}\wedge\mathrm{d}\Omega_3\wedge\mathrm{d}\rho, \tag{A9}$$

we get

$$\mathrm{d}C_{(8)} = \frac{\partial f}{\partial\phi}\mathrm{d}t\wedge\mathrm{d}\vec{x}\wedge\mathrm{d}\Omega_3\wedge\mathrm{d}y\wedge\mathrm{d}\phi - \frac{\partial f}{\partial\rho}\mathrm{d}t\wedge\mathrm{d}\vec{x}\wedge\mathrm{d}\Omega_3\wedge\mathrm{d}\rho\wedge\mathrm{d}y + \frac{\partial g}{\partial\phi}\mathrm{d}t\wedge\mathrm{d}\vec{x}\wedge\mathrm{d}\Omega_3\wedge\mathrm{d}\rho\wedge\mathrm{d}\phi + \frac{\partial g}{\partial y}\mathrm{d}t\wedge\mathrm{d}\vec{x}\wedge\mathrm{d}\Omega_3\wedge\mathrm{d}\rho\wedge\mathrm{d}y. \tag{A10}$$

By comparing Eq. (A7), we get the condition for $f(\rho, y, \phi)$ and $g(\rho, y, \phi)$ as follows:

$$\frac{\partial f}{\partial\phi} = -\frac{4q\rho^4 y}{(\rho^2+y^2)^3}, \qquad \frac{\partial g}{\partial\phi} = \frac{4q\rho^3 y^2}{(\rho^2+y^2)^3}, \qquad \frac{\partial f}{\partial\rho} - \frac{\partial g}{\partial y} = 0. \tag{A11}$$

By integrating f and g with respect to ϕ, we get

$$f(\rho, y, \phi) = -\frac{4q\rho^4 y}{(\rho^2+y^2)^3}(\phi+\phi_1), \qquad g(\rho, y, \phi) = \frac{4q\rho^3 y^2}{(\rho^2+y^2)^3}(\phi+\phi_2), \tag{A12}$$

but from the last condition of Eq. (A11), we get $\phi_1 = \phi_2 = \phi_0$. Finally, the 8-form potential can be written

$$C_{(8)} = -\frac{4q\rho^4 y}{(\rho^2+y^2)^3}(\phi+\phi_0)\mathrm{d}t\wedge\mathrm{d}\vec{x}\wedge\mathrm{d}\Omega_3\wedge\mathrm{d}y + \frac{4q\rho^3 y^2}{(\rho^2+y^2)^3}(\phi+\phi_0)\mathrm{d}t\wedge\mathrm{d}\vec{x}\wedge\mathrm{d}\Omega_3\wedge\mathrm{d}\rho. \tag{A13}$$

If we fix the location of the D7-brane along the ϕ direction at $\phi = \phi_*$, then Eq. (A13) becomes a total derivative, i.e.

$$C_{(8)} = -\frac{4q\rho^4 y}{(\rho^2+y^2)^3}(\phi_*+\phi_0)\mathrm{d}t\wedge\mathrm{d}\vec{x}\wedge\mathrm{d}\Omega_3\wedge\mathrm{d}y + \frac{4q\rho^3 y^2}{(\rho^2+y^2)^3}(\phi_*+\phi_0)\mathrm{d}t\wedge\mathrm{d}\vec{x}\wedge\mathrm{d}\Omega_3\wedge\mathrm{d}\rho = (\phi_*+\phi_0)\mathrm{d}\left[\frac{q\rho^4}{(\rho^2+y^2)^2}\mathrm{d}t\wedge\mathrm{d}\vec{x}\wedge\mathrm{d}\Omega_3\right], \tag{A14}$$

so that $C_{(8)}$ is a pure gauge whose field strength is zero. Furthermore, we can always choose $\phi_0 = -\phi_* + 2\pi$, then the Chern-Simons term in Eq. (3.3) becomes

$$S_{\mathrm{CS}} = \mu_7\int d^8\sigma(2\pi)\mathrm{d}\left[\frac{q\rho^4}{(\rho^2+y^2)^2}\mathrm{d}t\wedge\mathrm{d}\vec{x}\wedge\mathrm{d}\Omega_3\right] = (2\pi)\mu_7 V_4\Omega_3\frac{q\rho^4}{(\rho^2+y^2)^2}|_{\rho=\infty} = q(2\pi)\mu_7 V_4\Omega_3 = \frac{1}{2}N_{D(-1)}. \tag{A15}$$

It is nothing but the half of the D-instanton number calculated in Eq. [6]. This is completely satisfactory since the D7-brane world volume can capture the flux of the upper hemisphere. Since the Chern-Simons action is locally a total derivative term, it does not contribute to the equation of motion.

APPENDIX B: HAMILTONIAN DENSITY OF THE BARYON VERTEX

We start from the action for the D5-brane with the Chern-Simons term (4.7),

$$S_{D5} = S_{\mathrm{DBI}} + S_{\mathrm{CS}} = -\mu_5\int e^{-\Phi}\sqrt{-\det(g+2\pi\alpha' F)} + \mu_5\int A_{(1)}\wedge G_{(5)} = \tau_5\int dtd\theta\sin^4\theta\left[-\sqrt{e^{\Phi}\frac{\omega^2}{\omega_+}(\xi^2+\xi'^2)-\tilde{F}^2}+4\tilde{A}_t\right] = \int dtd\theta\,\mathcal{L}_{D5}, \tag{B1}$$

where

$$\tau_5 = \mu_5 \Omega_4 R^4 r_T, \qquad \tilde{F} = 2\pi\alpha' F_{t\theta}, \qquad \tilde{A}_t = 2\pi\alpha' A_t. \tag{B2}$$

We denote $\mathcal{L}_{D5}$ as Lagrangian density. The displacement can be obtained by a derivative of Lagrangian density with respect to A_t',

$$D(\theta) \equiv -\frac{\partial \mathcal{L}_{D5}}{\partial A_t'} = -2\pi\alpha'\tau_5 \frac{\sin^4\theta \tilde{F}}{\sqrt{e^{\Phi}\frac{\omega_-^2}{\omega_+}(\xi^2 + \xi'^2) - \tilde{F}^2}}. \tag{B3}$$

Then, the equation of motion for the gauge filed can be written as

$$\partial_\theta \hat{D}(\theta) = -4\sin^4\theta, \tag{B4}$$

where $\hat{D}(\theta) \equiv \frac{D(\theta)}{2\pi\alpha'\tau_5}$. This equation plays a constraint in the action; then, the action of the D5-brane becomes

$$\begin{aligned} S_{D5} &= S_{\mathrm{DBI}} + \tau_5 \int dt d\theta 4\sin^4\theta \tilde{A}_t \\ &= S_{\mathrm{DBI}} - \tau_5 \int dt d\theta (\partial_\theta \hat{D}(\theta)) \tilde{A}_t \\ &= S_{\mathrm{DBI}} - \tau_5 \int dt d\theta \hat{D}\, \tilde{F}, \end{aligned} \tag{B5}$$

where we take integration by part in the last procedure. This is nothing but the Legendre transformation of DBI action of the D5-brane. After substituting Eq. (B3) in the action, we define the Hamiltonian density (4.9) as follows:

$$\begin{aligned} S_{D5} &= -\tau_5 \int dt d\theta \sqrt{\frac{e^{\Phi}}{2}\frac{\omega_-^2}{\omega_+}(\xi'^2 + \xi^2)}\sqrt{\hat{D}(\theta)^2 + \sin^8\theta} \\ &\equiv -\int dt d\theta \mathcal{H}_{D5}. \end{aligned} \tag{B6}$$

The definition of Hamiltonian density is consistent with one of probe D7-brane, and integration of this with the on-shell solution gives free energy of the D5-brane. Next, by integrating Eq. (B4), we get

$$\hat{D}(\theta) = \frac{3}{2}(\nu\pi - \theta) + \frac{3}{2}\sin\theta\cos\theta + \sin^3\theta\cos\theta, \tag{B7}$$

where the integration constant ν determines the number of fundamental strings on each pole, i.e. νN_c strings are attached to the south pole and $(1-\nu)N_c$ strings to north pole of the D5-brane. Here, we assume that all the fundamental strings are attached on the north pole, and we set $\nu = 0$.

APPENDIX C: FORCE-BALANCE CONDITION

In this section, we derive the force-balance condition (4.11). In our mode, the end points of fundamental strings play a role of source of the $U(1)$ gauge field. Because of the tension of the fundamental string, there can exist cusps on probe-brane world volume. By calculating force at the cusp of each brane, we can estimate the behavior of probe branes.

The force at the cusp can be obtained by taking small variations of "on-shell" free energy with respect to U_c,

$$F_c = \frac{\delta \mathcal{F}_{\text{on-shell}}}{\delta U_c}, \tag{C1}$$

where U_c is the position of the cusp and the free energy is the integration of Hamiltonian density of the probe brane,

$$\mathcal{F} = \int d\rho \mathcal{H}_{\text{on-shell}}. \tag{C2}$$

The Hamiltonian density is a function of U and U'. We can write the variation as follows:

$$\begin{aligned} \delta\mathcal{H}_{\text{on-shell}} &= \delta\mathcal{H}(U, U'; \rho)_{\text{on-shell}} = \frac{\partial \mathcal{H}_{\text{on-shell}}}{\partial U}\delta U + \frac{\partial \mathcal{H}_{\text{on-shell}}}{\partial U'}\delta U' \\ &= \frac{\partial \mathcal{H}_{\text{on-shell}}}{\partial U}\delta U + \frac{d}{d\rho}\left[\frac{\partial \mathcal{H}_{\text{on-shell}}}{\partial U'}\delta U\right] - \frac{d}{d\rho}\left(\frac{\partial \mathcal{H}_{\text{on-shell}}}{\partial U'}\right)\delta U \\ &= \frac{d}{d\rho}\left[\frac{\partial \mathcal{H}_{\text{on-shell}}}{\partial U'}\delta U\right] + \left[\frac{\partial \mathcal{H}_{\text{on-shell}}}{\partial U} - \frac{d}{d\rho}\left(\frac{\partial \mathcal{H}_{\text{on-shell}}}{\partial U'}\right)\right]\delta U = \frac{d}{d\rho}\left[\frac{\partial \mathcal{H}_{\text{on-shell}}}{\partial U'}\delta U\right]. \end{aligned} \tag{C3}$$

Finally, the force at the cusp is

$$\begin{aligned} F_c &= \int d\rho \frac{\delta \mathcal{H}_{\text{on-shell}}}{\delta U_c} = \int d\rho \frac{d}{d\rho}\left[\frac{\partial \mathcal{H}_{\text{on-shell}}}{\partial U'}\frac{\delta U}{\delta U_c}\right] \\ &= \frac{\partial \mathcal{H}_{\text{on-shell}}}{\partial U'}\bigg|_{U=Uc}. \end{aligned} \tag{C4}$$

The force at the cusp of the single D5-brane can be calculated from Eq. (C4),

$$F_{D5} = N_c T_{F1}\sqrt{\frac{e^{\Phi}}{2}\frac{\omega_-^2}{\omega_+}}\frac{\xi'}{\sqrt{\xi^2 + \xi'^2}}\bigg|_{\xi=\xi_c}, \tag{C5}$$

where T_{F1} is the tension of fundamental string $1/2\pi\alpha'$ and ξ_c is the position of the cusp of the D5-brane. With a same manner, we can get the force at the cusp of the probe D7-brane,

$$F_{D7} = T_{F1}\sqrt{\frac{e^{\Phi}}{2}}\frac{\omega_-^2}{\omega_+}\frac{Q\dot{y}}{\sqrt{1+\dot{y}^2}}\Big|\, y = y_c, \tag{C6}$$

where y_c is the position of the D7-brane at the cusp ($\rho = 0$) and Q is total number of the $U(1)$ source. The force at the cusp of D5 and D7 is always smaller than the fore of fundamental strings. Then, strings pull each brane until the length of the string becomes zero and force between two branes is balanced. We can get the condition of slope of the D7-brane from the force-balance condition.

$$\begin{aligned} 0 &= F_{D7}(Q) + N_B F_{D5} \\ &= F_{D7}(Q) + \frac{Q}{N_c}F_{D5} \\ &\rightarrow \\ \dot{y}_c &= \frac{\xi_c'}{\xi_c}. \end{aligned} \tag{C7}$$

[1] E. Witten, Adv. Theor. Math. Phys. **2**, 505 (1998).
[2] E. Witten, J. High Energy Phys. 07 (1998) 006.
[3] C. G. Callan, A. Guijosa, K. G. Savvidy, and O. Tafjord, Nucl. Phys. **B555**, 183 (1999).
[4] Y. Seo and S. J. Sin, J. High Energy Phys. 04 (2008) 010.
[5] T. Schafer and E. V. Shuryak, Rev. Mod. Phys. **70**, 323 (1998).
[6] H. Liu and A. A. Tseytlin, Nucl. Phys. **B553**, 231 (1999).
[7] K. Ghoroku, T. Sakaguchi, N. Uekusa, and M. Yahiro, Phys. Rev. D **71**, 106002 (2005).
[8] S. S. Gubser, Phys. Rev. D **80**, 1015016 (2009).
[9] Y. Kim, B. H. Lee, C. Park, and S. J. Sin, Phys. Rev. D **80**, 105016 (2009).
[10] K. Y. Kim, S. J. Sin, and I. Zahed, arXiv:hep-th/0608046.
[11] N. Horigome and Y. Tanii, J. High Energy Phys. 01 (2007) 072.
[12] S. Nakamura, Y. Seo, S. J. Sin, and K. P. Yogendran, J. Korean Phys. Soc. **52**, 1734 (2008); Prog. Theor. Phys. **120**, 51 (2008).
[13] S. Kobayashi, D. Mateos, S. Matsuura, R. C. Myers, and R. M. Thomson, J. High Energy Phys. 02 (2007) 016; D. Mateos, S. Matsuura, R. C. Myers, and R. M. Thomson, J. High Energy Phys. 11 (2007) 085.
[14] K. Ghoroku and M. Ishihara, Phys. Rev. D **77**, 086003 (2008).
[15] S. J. Sin and Y. Zhou, J. High Energy Phys. 05 (2009) 044.
[16] G. W. Gibbons, M. B. Green, and M. J. Perry, Phys. Lett. B **370**, 37 (1996).
[17] A. Kehagias and K. Sfetsos, Phys. Lett. B **456**, 22 (1999).
[18] K. Ghoroku and M. Yahiro, Phys. Lett. B **604**, 235 (2004).
[19] M. Kruczenski, D. Mateos, R. C. Myers, and D. J. Winters, J. High Energy Phys. 07 (2003) 049.
[20] J. Babington, J. Erdmenger, N. J. Evans, Z. Guralnik, and I. Kirsch, Phys. Rev. D **69**, 066007 (2004).
[21] M. Kruczenski, D. Mateos, R. C. Myers, and D. J. Winters, J. High Energy Phys. 05 (2004) 041.
[22] J. Erdmenger, A. Gorsky, P. N. Kopnin, A. Krikun, and A. V. Zayakin, J. High Energy Phys. 03 (2011) 044.
[23] M. A. Shifman, A. I. Vainshtein, and V. I. Zakharov, Nucl. Phys. **B147**, 385 (1979).
[24] D. Mateos, R. C. Myers, and R. M. Thomson, Phys. Rev. Lett. **97**, 091601 (2006).J. High Energy Phys. 05 (2007) 067.
[25] N. Evans, A. Gebauer, K. Y. Kim, and M. Magou, J. High Energy Phys. 03 (2010) 132.
[26] O. Bergman, G. Lifschytz, and M. Lippert, J. High Energy Phys. 11 (2007) 056.
[27] O. Aharony, J. Sonnenschein, and S. Yankielowicz, Ann. Phys. (Leipzig) **322**, 1420 (2007).
[28] M. Bianchi, M. B. Green, S. Kovacs, and G. Rossi, J. High Energy Phys. 08 (1998) 013.
[29] N. Dorey, T. J. Hollowood, V. V. Khoze, M. P. Mattis, and S. Vandoren, Nucl. Phys. **B552**, 88 (1999).